Line-shape effects on the determination of Coster-Kronig probabilities using Si(Li) x-ray detectors

T. Papp,[1,2] J. L. Campbell,[1] and S. Raman[3]
[1]*Guelph-Waterloo Program for Graduate Work in Physics, University of Guelph, Guelph, Ontario, Canada N1G 2W1*
[2]*Institute of Nuclear Research of the Hungarian Academy of Sciences (ATOMKI) Debrecen, H-4001, Pf.51 Hungary*
[3]*Oak Ridge National Laboratory, Oak Ridge, Tennessee 37831*
(Received 26 August 1993)

The great majority of measured values of the Coster-Kronig probability f_{23} derive from x-ray coincidence experiments using radionuclide sources or from synchrotron-radiation excitation of thin foils. Very little attention has been paid in published work to the role of line-shape effects and satellites in the x-ray spectra that are obtained. It is shown that this neglect can influence f_{23} values derived from such measurements. This may explain in part the well-established trends for measured f_{23} values to fall below the theoretical predictions for elements with atomic number $Z < 90$ and to fall above when $Z > 92$. In elemental analysis techniques based upon x-ray emission spectroscopy, where a database of atomic parameters such as Coster-Kronig probabilities is used, the same approximations are made in treating the spectra. Until a more sophisticated approach to spectrum reduction is developed, it may be preferable in this context to use "nominal" Coster-Kronig probabilities derived from experiment in preference to theoretical values.

PACS number(s): 32.30.Rj, 34.50.Fa, 32.80.Hd

I. INTRODUCTION

Atomic parameters such as proton-induced subshell ionization cross sections, subshell x-ray fluorescence yields, and Coster-Kronig and radiative transition probabilities form a data base that is important in many applications. Much experimental effort has been expended in attempts to improve our knowledge of Coster-Kronig (CK) transition probabilities for the L subshells [1]. The two main streams of experimental information were obtained by the synchrotron ionization method [2–4] and the K-L x-ray coincidence method [5–7]. In both methods the x rays were detected by Si(Li) detectors, and in each case the references cited previously are illustrative rather than exhaustive. The purpose of this paper is to examine the influence of three factors that have hitherto been ignored in the interpretation of data from these techniques. The first factor is the intrinsic Lorentzian energy distribution within a given x-ray line; the second is the satellite contribution to the x-ray spectra; and the third is the low-energy tail in the Si(Li) detector response function.

II. OVERVIEW OF PREVIOUS EXPERIMENTS

The K-L x-ray coincidence technique uses two x-ray detectors. The first of these, usually a Ge detector, records the K x-ray spectrum from a thin deposit of a radionuclide whose decay involves orbital electron capture, internal conversion, or both processes. The energy resolution is such that the $K\alpha_1$ and $K\alpha_2$ x rays, which signify, respectively, L_3 and L_2 vacancies, are well separated. The second detector, usually a Si(Li) detector, records the L x rays that are emitted in coincidence with $K\alpha_1$ and $K\alpha_2$ in the first detector. The fraction of L_3 x rays observed in the spectrum coincident with L_2 vacancy signals then provides a measure of the CK vacancy transfer probability f_{23}. Recent results from this method have tended to converge and the overall trend (see Fig. 1) is for the experimental data in the well-studied atomic number region $60 < Z < 90$ to lie some 10% below the predictions of the Dirac-Hartree-Slater (DHS) model [8].

Because the K-L_1 x-ray line is $E1$ forbidden, this method does not generate an equally useful indicator of L_1 vacancies. While there do exist radionuclide studies of the L_1 CK probabilities f_{12} and f_{13}, they are few and the experimental errors are large. This has made the synchrotron ionization method an attractive alternative. Here L x-ray spectra are recorded from a thin foil bombarded by a beam of monoenergetic photons from a syn-

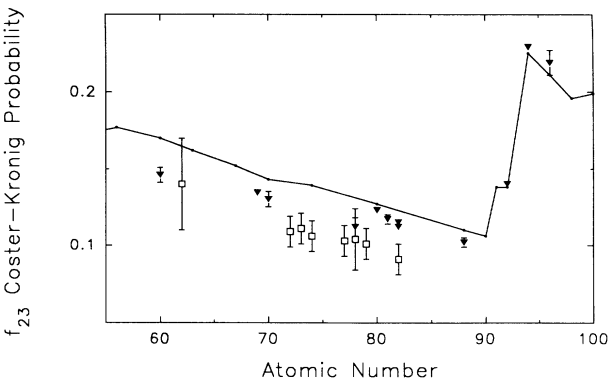

FIG. 1. f_{23} Coster-Kronig probabilities. Experimental data: ▼, K-L coincidence technique [5,6]; □, synchrotron photoionization method [2,4]. The line represents the DHS calculations of Chen *et al.* [8].

chrotron storage ring. The photon energy is stepped through a series of values such that it crosses the three L subshell absorption edges. When the energy is sufficient to create vacancies only in the L_3 subshell, the observed spectrum comprises L_3 x rays only. As the energy is moved above the L_2 edge, L_2 x rays are absorbed and the L_3 x-ray intensity is augmented since some of the L_2 vacancies are transferred to the L_3 subshell by the CK process; the increase in L_3 x-ray intensity gives the quantity f_{23}. Similarly, as the photon energy crosses the L_1 threshold, L_1 x rays appear, but the L_3 intensity is again augmented as L_1 vacancies are shifted by the CK process to L_2 and L_3. Jitschin and various co-workers [2–4] measured the L subshell CK probabilities for a large number of Z values. Their results for f_{23} are internally consistent, but they fall some 20% below the DHS predictions [8] and are systematically different from the results of the K-L x-ray method.

In neither method has attention been paid to the fact that the result of a CK transition is a double vacancy state, which will deexcite through various decay channels, with the resulting x-ray spectrum containing very many satellite transitions. The peculiarity of x-ray spectra emitted after vacancies have been shifted to higher subshells by the CK process is that the main contribution arises from satellites. It has been implicitly assumed, because the energy resolution of the Si(Li) detectors is much greater than the energy spread due to any satellite structure, that such structure could be ignored in analyzing the spectra. However, the claimed experimental accuracy of f_{23} measurements has reached the 1–5% level [5,6], where hitherto ignored line-shape effects may cause a comparable systematic error.

When the L_2-L_3M CK channels are open, the x-ray spectra contain LM satellites whose energy separation from the diagram line (singly ionized atom transition) can be as large as 50–60 eV for uranium L_3 x rays [9], while the detector resolution is around 200–250 eV. This spreading out of the studied transition impacts differently upon the K-L coincidence technique and the impact ionization technique. In the $K\alpha_2$-L coincidence spectrum, the $L\alpha$ satellite compound is fitted by a Gaussian function, which may be broader than the detector resolution and can have a different centroid than the diagram line. In the case of impact ionization, the spectrum consists predominantly of the diagram line on which is superposed a small contribution (5–10%) of satellite spectrum. Here the Gaussian width and the centroid energy will be determined predominantly by the diagram line spectrum, and the resulting values will not be precisely appropriate for the superimposed satellite contribution.

III. BASIS OF THE CURRENT STUDY

This work investigates how the peak area determined from a Si(Li) detector spectrum depends on the different model assumptions for the satellite structure and detector line-shape effects. We used the K-L coincidence technique to generate various x-ray spectra from two radionuclide sources. The K-L coincidence technique has the drawback that only the f_{23} CK transition probabilities can be determined. Because in both the synchrotron ionization method and the K-L coincidence method the f_{23} parameter is determined from the $L\alpha$ line intensities, we concentrated on the $L\alpha$ line only. The K-L coincidence technique has the advantage that selection of the $K\alpha_1$ transition by the coincidence window results in only the diagram line occurring in the L_3 spectrum; similarly, selecting the $K\alpha_2$ transition results in only the CK satellite spectrum being present in the L_3 spectrum. By summing these two types of spectrum in proper proportion, it is possible to generate a spectrum similar in composition to the synchrotron ionization spectrum excited by radiation whose energy exceeds the $L2$ binding energy.

It is not the intent of the paper to present new experimental values of the CK probability. The radionuclides used in our work would not be particularly good choices for accurate f_{23} measurements. Rather they were chosen on grounds of their suitability for illustrating in a quantitative fashion the various effects that conspire to introduce error into existing experimental data.

IV. EXPERIMENT

In the K-L coincidence method, only 5–10% of the real coincidence events originate from the K-L_2-(L_3,M,N,O,...) cascade transitions, while reasonably high statistics are necessary to study the line-shape effects. A long measuring time is therefore required. In our earlier study [10] on K-L angular correlations in uranium, we collected many coincident events as a function of the detection angle in list mode; therefore, we have simply appended these data files to produce a single large file having excellent statistics. Although we cannot determine the f_{23} parameter from this extended file because the $K\alpha_1$-$L\alpha$ cascade has angular correlation, the high statistics nevertheless enable us to study the effect of the line-shape models.

We carried out measurements on two radionuclides. It was desirable to choose one where the L_2-L_3M CK channels are energetically allowed. We selected uranium (as indicated above), where the L_2-L_3M_5 channel is allowed while the other M channels are blocked. The other case studied was gadolinium, where the M channels are not allowed, the separation of the x-ray lines is not very large, and the low-energy tail in the Si(Li) detector response function may play a role in the analysis.

The uranium x rays were obtained from the radionuclide $^{233}_{91}$Pa, which decays by internal conversion of nuclear electromagnetic transitions to $^{233}_{92}$U with a 27-day half-life. The source was prepared by a 50-h thermal neutron irradiation (flux 2×10^{13} neutrons $s^{-1}cm^2$) of 1-mg/cm^2-thick metallic thorium foil having an area of 6 mm^2. This irradiation produces the radionuclide ^{233}Th, which decays with a 22-min half-life to ^{233}Pa. The thorium matrix will give thorium x-ray lines via secondary fluorescence by uranium x rays and β particles, but these thorium lines are well separated in energy from the uranium lines.

The gadolinium x rays were provided by a $^{157}_{65}$Tb source which decays by electron capture predominantly to $^{157}_{65}$Gd with a half-life of 100 yr. The starting point was ^{157}Dy (8

h) produced by irradiating for 1 week approximately 20 mg of 20.5% enriched ^{156}Dy in a flux of 2.5×10^{15} neutrons $s^{-1}cm^{-2}$. After allowing ^{157}Dy to decay to ^{157}Tb, terbium was separated from dysprosium through high-pressure ion exchange. After converting the terbium fraction to a solid form, the material was passed through an isotope separator to implant ^{157}Tb in a thin aluminum foil.

Two detectors viewed the source. The L x rays were detected by a Si(Li) detector manufactured by Link Analytical. The Si(Li) crystal is nominally 3 mm thick and an internal collimator restricts its effective diameter to 5 mm. An additional external collimator 3 mm in diameter was used to restrict the x rays to the central region of the detector area. This detector has a beryllium window of thickness 0.008 mm and detector energy resolution at 5.9 keV of 133 eV [full width at half maximum (FWHM)]. The K x rays were detected by a high-purity germanium detector (HpGe) fabricated by Aptec Inc. It has a thickness of 10 mm and a diameter of 20 mm. It is equipped with a 0.5-mm beryllium window of unusually large diameter, 75 mm, which forms the entire front face of the cryostat, thus minimizing the scattering of K x rays and subsequent degraded events in the spectrum. The energy resolution was 530 eV at 122 keV. The detector distances were 6.1 and 3.6 cm, respectively, for the uranium measurements and 3.6 and 2.1 cm, respectively, for the gadolinium measurements. These two detectors were chosen for their excellent line-shape characteristics, which in each case have been discussed elsewhere [5,11–13]. In the uranium experiment a copper absorber was placed in front of the HpGe detector to diminish the intensity of L x rays, and a 0.37-mm-thick Mylar $(C_{10}H_8O_4)_x$ absorber was placed in front of the Si(Li) detector to block the β particles. In the gadolinium experiment an aluminum absorber of thickness 0.25 mm was placed in front of the HpGe detector. The uranium measurement consisted of 12 runs performed at 10 angles during a 5-month continuous measurement in the range of 90°–180°. In the gadolinium measurement one single long run of duration of 11 d was performed during which the two detectors were in close proximity at 180°. The electronic coincidence system is described in Ref. [10], and all the coincidence events were stored on disk in list mode.

V. DATA EVALUATION

A. Overview

From the uranium data stored in list mode, several spectra were reconstructed, using windows established on the K, L, and T (time) spectra [10]. Our main interest was to generate L-shell spectra in coincidence with the $K\alpha_1$ and $K\alpha_2$ lines. The L spectra obtained after subtracting the random coincidences with the aid of the real- and random-time window spectra were further corrected for contributions other than those arising from successive K and L x-ray emission in a given atom. Some of the electromagnetic transitions in the daughter ^{233}U nucleus are in cascades and in this way K and L x rays from sequential internal conversions are recorded as coincidences [10]. We refer to the nuclear cascade contributions as unrelated coincidences, which include additionally the secondary x rays arising from fluorescence or β-particle ionization. The spectra were corrected for these events as described in Ref. [10]. The $K\alpha_1$ and $K\alpha_2$ lines are well separated in the case of uranium, and the derivation of the L spectra is straightforward.

For gadolinium x rays measured by the present germanium detector, the $K\alpha_1$ and $K\alpha_2$ lines have significant overlap (see Fig. 2) and therefore we established windows on only appropriate parts of the lines. The $K\alpha_2$ window extends from the low-energy point on the left-hand side where the $K\alpha_2$ peak has fallen to 1% of its height to the point where the $K\alpha_1$ peak has fallen (on its left) to 1% of its height; the latter point was defined by reflecting the right-hand 1% of height point through the $K\alpha_1$ peak centroid. The purpose of these windows is simply to maximize the contributions, respectively, of L_2 and L_3 vacancy events in each.

The L x-ray spectrum in coincidence with the $K\alpha_1$ radiation originates from the filling of L_3 vacancies basically in the singly ionized atoms emitting L_3 diagram lines. The L x-ray spectrum in coincidence with the $K\alpha_2$ radiation contains L_2 diagram lines and, because of the CK processes, L_3 x-ray lines will also be present. However, these L_3 x rays originate from filling the L_3 vacancy in doubly ionized atoms. In this manner the spectra arising from singly and doubly ionized atoms are separated and can be studied independently.

B. Analysis of uranium spectra

A range of the $K\alpha_1$-L spectrum (Fig. 3), containing the $L\alpha$ lines of uranium and thorium, was analyzed. Two nonlinear least-squares fits were performed. In the first

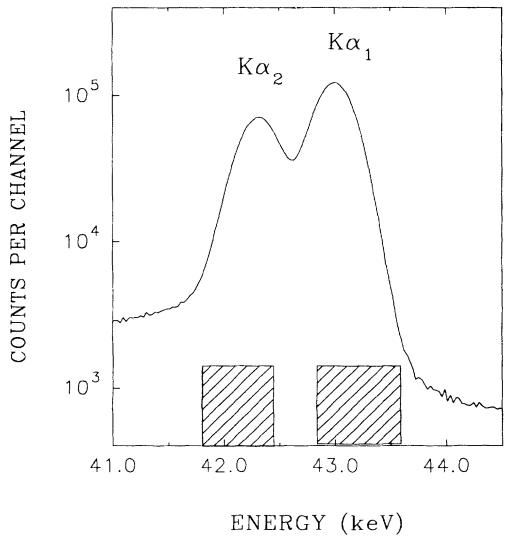

FIG. 2. $K\alpha$ spectrum of gadolinium recorded by a high-purity germanium detector. The $K\alpha_2$ and $K\alpha_1$ windows for the generation of the L spectra in coincidence with the $K\alpha_2$ and $K\alpha_1$ radiation are marked with shaded regions.

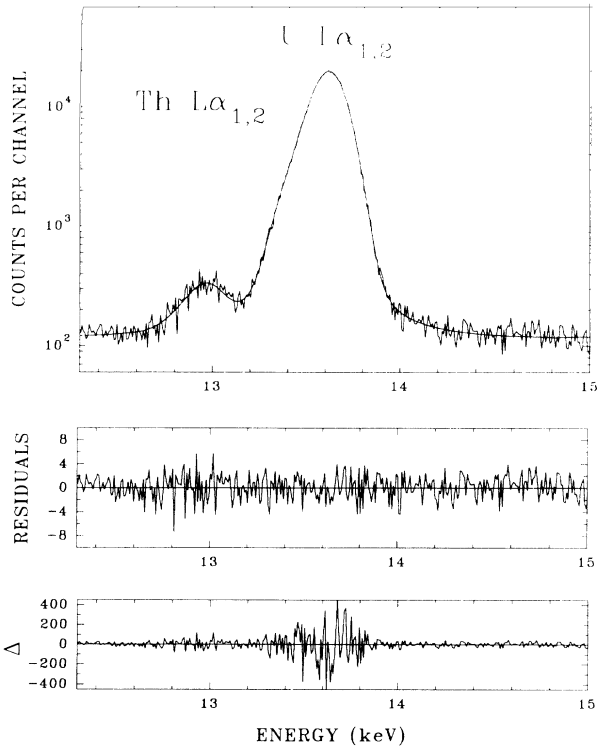

FIG. 3. Details of the fit to the region of the uranium L x-ray spectrum, containing uranium and thorium $L\alpha$ lines, in coincidence with the $K\alpha_1$ radiation. The full curve in the upper section represents the fit. The residuals are in units of one standard deviation. Δ represents the difference between measured and fitted spectra.

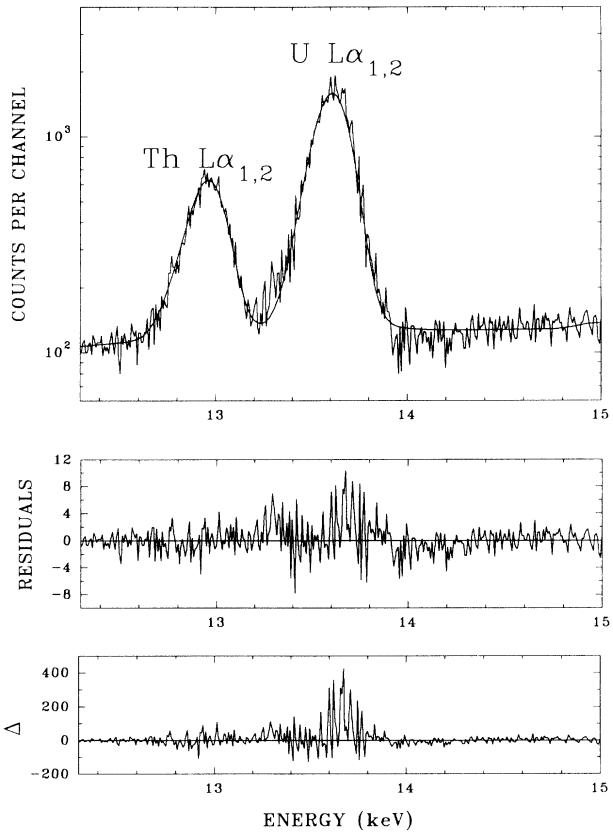

FIG. 4. Details of the fit to the region of the uranium L x-ray spectrum in coincidence with the $K\alpha_2$ radiation. The full curve in the upper section is the fit obtained with the same line parameters (energy calibration, Gaussian and Lorentzian widths, tail parameters) fixed at the values generated in the fit of Fig. 3, that is, fixed at the values pertinent to the spectrum in coincidence with $K\alpha_1$. Residuals and differences are as defined for Fig. 3.

the line shape was modeled as a Gaussian function with low-energy tailing features (an exponential tail, a flat shelf extending to low photon energies, and a truncated flat shelf) which were determined earlier [11,12]. This fit did not give fully satisfactory results because the natural line shape of the electromagnetic transition (Lorentzian) was neglected. Because a very long (5-month duration) measurement was carried out, our spectra had unusually good statistics with about 10^6 counts in the $L\alpha_{1,2}$ peak in coincidence with the $K\alpha_1$ line. In the more usual coincidence measurements having significantly lower statistics, the need for Lorentzian broadening is not obvious and has invariably been neglected, therefore resulting in a systematic deviation. In our second fit to the $K\alpha_1$-$L\alpha$ spectrum, the Lorentzian line shape was convoluted with the detector response function. The results of this fit are presented in Fig. 3. This fit gave a 4% larger area for the $L\alpha_{1,2}$ peak than in the first fit, and consequently a 4% increase in the number of the $K\alpha_1$-$L\alpha_{1,2}$ coincidence events. From this second fit the energy calibration and the detector Gaussian width calibration were determined.

Performing the same fit as in the case of Fig. 3 (with the energy and width calibrations fixed at the values determined above) for the same $L\alpha$ range in coincidence with the $K\alpha_2$ events, it became obvious that the FWHM of the peak was in this case broadened and that the centroid of the peaks were shifted. We will refer to this fit as fit 3 (see Fig. 4). When the peak energy and width calibration parameters were released and allowed to be variables of the fit (referred to as fit 4), the energy shifts of the peak centroids were found to be 15 eV for the $L\alpha_2$ and 13 eV for the $L\alpha_1$ transitions (Fig. 5). The area obtained was 7.5% larger than that obtained in fit 3, and the residuals were much smaller, indicating a better fit. When fit 4 was repeated with the Lorentzian neglected, there was little change in the outcome. Thus in this spectrum the shifted and variable $L\alpha_1$ and $L\alpha_2$ peak energies and broader Gaussian functions apparently compensated in a somewhat crude fashion for the neglect of the Lorentzian tail contribution.

Even with the improvements conferred by the above procedure, this model of the $K\alpha_2$-L_2 coincidence spectrum is not expected to be fully appropriate because the detailed satellite structure of the peaks was not invoked in the evaluation. It is possible to make an approximate model for the x-ray spectrum of these two vacancy states using calculated L_2-L_3X CK transition probabilities [14] and satellite transition energies [9]. To simulate the spectrum we need additionally the transition probabilities and the Lorentzian widths of the transitions. We found in the literature two assumptions that are relevant to this problem. One of them takes the x-ray transition probability to

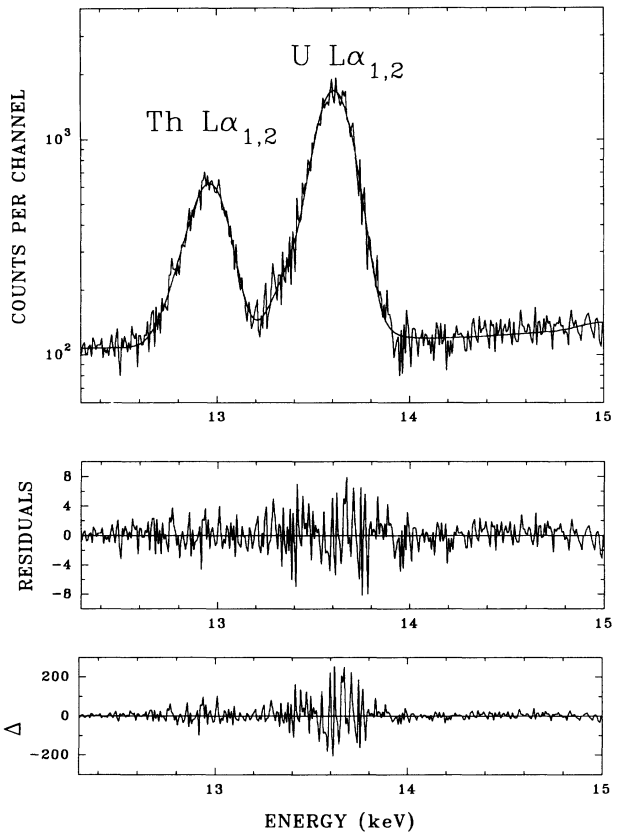

FIG. 5. The analog of Fig. 4, except that the line energies and Gaussian widths are free parameters of the fit. Note the different scale for the residuals and Δ.

be the same as in the case of singly ionized atoms [2,4–7,15,16]. Because the transition probability is proportional to the number of vacancies and the number of electrons in the participating shells [17], these quantities may have a first-order effect on the transition probabilities as was demonstrated in Ref. [18]. This may be of interest when the CK transition probabilities are determined using transitions where the inner vacancy is filled by an electron from an upper level in which there is a preexisting vacancy. An example is the $L\alpha_{1,2}$ transition when the L_1-$L_3M_{5,4}$ or the L_2-$L_3M_{5,4}$ channels are energetically allowed, or the $L\gamma 1$ transition when the L_1-L_2N_4 channel has a large rate. No assumption was found concerning the Lorentzian widths of such transitions in Refs. [2,4–7,15], while it was assumed in Ref.[16] that the second (i.e., spectator) vacancy has infinite lifetime or, in other words that the energy level corresponding to the vacancy is infinitely sharp. Another assumption that we think is a more accurate approximation was described in detail in the pioneering work of Richtmyer and Ramberg [19]. They assumed that the satellite Lorentzian width is the sum of the initial and final level widths and that the double-vacancy level width is the sum of the two corresponding single-vacancy level widths; thus, for example,

$$\Gamma(L_3M_5\text{-}M_xM_5)=[\Gamma(L_3)+\Gamma(M_5)]+[\Gamma(M_x)+\Gamma(M_5)]\ . \quad (1)$$

Although this is an approximation, we followed the procedure described in Ref. [19] to model the x-ray satellite spectra.

For uranium, 30% of the f_{23} CK transitions proceed via the L_2-L_3M_5 channel and most of the remaining transitions through the L_2-L_3N channel. For the L,M,N level widths we assumed the widths reported in Ref. [20]. For the satellite energies and relative intensities we used the information of Refs. [9,14]. The energy and intensity distributions of the satellites are shown in Fig. 6 for the $L\alpha_1$ transition; they are very similar for the $L\alpha_2$ transition. The zero energy shift corresponds to those transitions where the second vacancy decays first, and the vacancy was transferred to shells higher than the N shells. For this we used the diagram line energy and Lorentzian width.

The relative strength of the satellite in a given multiplet splitting was calculated by using Eq. (6) of Ref. [9]. The relative strength of the summed M shell satellites relative to the N or higher shell satellite intensities was a fitting parameter of the fit. In this manner the modification in the M_5-L_3 transition rates because of the partially filled M_5 shell was involved in the fitting process. The $La_{1,2}$ peak area thus obtained was 8% larger than in fit 3. This is essentially the same outcome as that of fit 4 and it indicates that the satellite energy shift does indeed cause a larger effect than the Lorentzian broadening. It also indicates that the crude analysis of fit 4 actually gives a quite satisfactory outcome.

In the K-L coincidence method, the f_{23} probability is obtained from the ratio of $L\alpha$ x-ray intensities in the K-L_2 and K-L_3 coincidence spectra. These intensities are customarily obtained by simple Gaussian fits in which the peak positions and widths are variables. From the calculations above we conclude that our analysis including Lorentzian and detector response function effects increase the La intensity in coincidence with $K\alpha_1$ by 4% relative to the conventional fit with Gaussian functions; however, the simple Gaussian fit gives much the same results as our more sophisticated analysis for the $L\alpha$ intensity in coincidence with $K\alpha_2$. The overall result of our

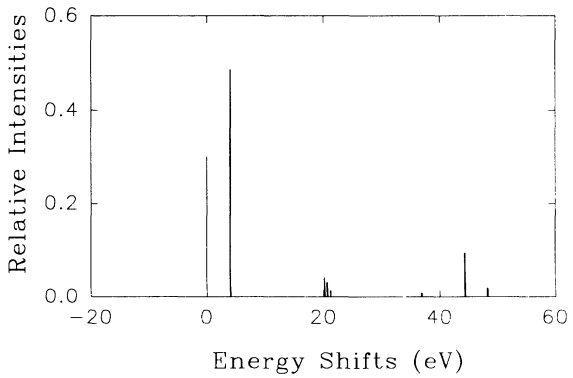

FIG. 6. The energies and intensities of the Coster-Kronig satellites of the uranium $L\alpha_1$ transition as determined from the model of Ref. [14]. The zero energy corresponds to the diagram line.

approach is an f_{23} value for uranium that is 4% lower than that given by the conventional analysis.

Turning to photoionization, the measured spectrum in this case would be a sum of two spectra of the type described in the preceding paragraphs. To simulate this situation for uranium we added together the $K\alpha_1$-L and $K\alpha_2$-L spectra in proper proportion and fitted the $L\alpha$ region of the sum spectrum in the same manner as in fit 4, that is, the Lorentzian broadening was included and the energy and width parameters were variables of the fit. After thus determining the $L\alpha$ peak area in the sum spectrum, we subtracted the L_α area determined by fitting the $K\alpha_1$-$L\alpha$ coincidence spectrum (fit 2); the remaining $L\alpha$ peak intensity was 4.5% less than the value obtained by fitting the La spectrum in coincidence with the $Ka2$ coincidence spectrum (fit 4). This 4.5% discrepancy increased to 6% when the Lorentzian broadening was neglected in this procedure. Thus the current analysis of photoionization data in this simulated experiment would produce an f_{23} result 6% higher than the conventional analysis which neglects line-shape effects.

We have shown that for atoms having atomic number $Z > 92$ the conventional analysis produces results that are 4% high in the coincidence method and 6% low in the photoionization method.

C. Analysis of gadolinium spectra

In the case of gadolinium the L x-ray peaks are less well resolved even using this very good resolution and low tail characteristic detector. The $K\alpha_1$-L and $K\alpha_2$-L coincidence spectra are shown in Fig. 7. The $L\alpha$ peak is the main peak in the $K\alpha_1$-L spectrum, while the $K\alpha_2$-L spectrum is dominated by the $L\beta_1$ (L_2-M_4) peak. In the latter case the fitting of the $L\alpha$ peak (with only 50 000 counts intensity) will be strongly influenced by the low-energy tail of the nearby $L\beta_1$ peak (200 000 counts in intensity); this tail is represented by the full line in Fig. 7(b). In the K-L coincidence measurements [5–7], the f_{23} probability was determined by fitting the $L\alpha$ peak with a Gaussian function. At first we fitted the spectra in the same way, where only the $L\alpha$ peak region was fitted by a Gaussian function and a linear background. In the next step we fitted the spectra involving the entire Ll, $L\alpha$, and $L\beta$ complex. Every peak was represented by a Lorentzian function convoluted with the detector response function (a Gaussian function with low-energy tailing). This analysis resulted in 1% larger f_{23}, which arises mainly from the different background model under the $L\alpha$ peak.

The method of analysis of the gadolinium spectra in terms of satellites is different from the procedure described previously for the uranium spectra because here the $L_2L_3M_i$ Coster-Kronig channels are energetically forbidden. The satellites are due to N rather than M spectator vacancies and are very close in energy to the diagram lines. For gadolinium, the $L\alpha$ satellites all lie within 7 eV of the diagram line. Indeed for the majority of them the separation is less than 3 eV, a value which is negligible compared to the detector resolution; however, because it is comparable with the natural width of the doubly ionized states, the satellites merit further consideration. The main CK channels are the L_2-L_3N_2 and L_2-L_3N_4 transitions. The energy differences of the different multiplets of the L_3N_2 or L_3N_4 double ionized states of gadolinium are smaller than the widths of these states, and in these cases the multiplet formation is incomplete. For the L_3N_3 vacancies the multiplet formation is almost complete. The multiplet splitting is larger for the M_5N_i and M_4N_i states, which are the final vacancy states of the studied $L\alpha_{1,2}$ transitions, but the multiplet formation is still incomplete. To build up a model like that described above for uranium the decay scheme of the doubly ionized states including the N subshells would be necessary. Because this detailed information was not available, we took the following simple approach. The $L\alpha_{1,2}$ peak was modeled with two lines corresponding to its two components, the energies being set equal to the diagram-line energies. First the Lorentzian widths were taken to be the same as in the singly ionized atoms (4.3 eV for both $L\alpha$ transitions). When we used twice larger values for the Lorentzian widths to approximate the effect of the spectator vacancies, this increased the value of f_{23} by 3% relative to the value based on the first Lorentzian-width estimate.

At the end of this analysis, we can conclude that the neglect of the various line-shape effects in an f_{23} measurement conducted with the present detector would result in a 1–4 % error in the downward direction. The inclusion of these effects would bring the f_{23} closer to theory.

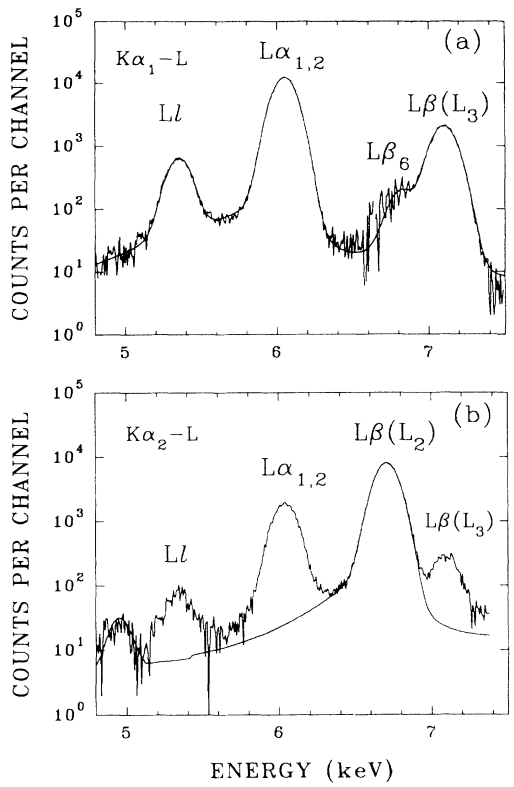

FIG. 7. The $L1$-$L\alpha$-$L\beta$ range of the gadolinium spectra in coincidence with the (a) $K\alpha_1$ and (b) $K\alpha_2$ transitions. The lower portion shows the fitted lineshape of the $L\beta_1(L_2$-$N4)$ transition.

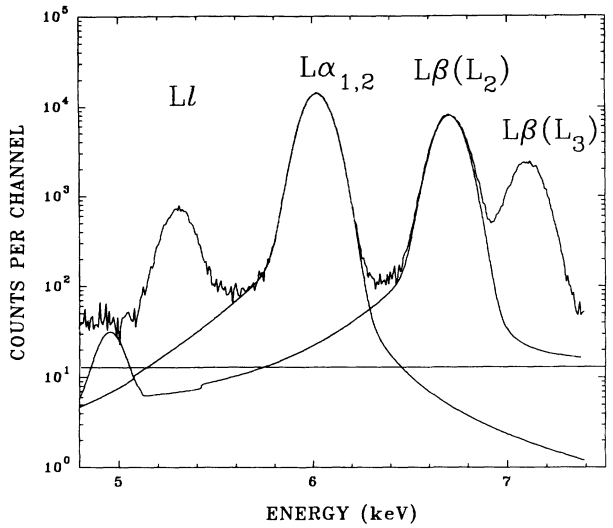

FIG. 8. The spectrum presented here was obtained by adding together the measured spectra shown in Figs. 7(a) and 7(b). The line shapes of the $L\alpha_{1,2}$ and the $L\beta_1$ transitions along with the best fit using a constant background are also presented to demonstrate the interplay between the different components of the fit.

As in the uranium example, summing the two coincidence spectra is expected to produce a spectrum similar to that produced by photoionization. We assumed a constant background, and the range in the vicinity of the $L\alpha$ was fitted for the $K\alpha_1$-L, the $K\alpha_2$-L, and the summed spectra. From the three fits the intensities of the $L\alpha$ peaks were determined. Following the same analysis for photoionization as in the uranium case, we can determined the $L\alpha$ intensity originating from L_2 vacancies by subtracting the $K\alpha_1$-$L\alpha$ coincidence intensity from the summed spectrum $L\alpha$ line intensity. The resulting value was 3% less than the directly fitted intensity in the measured $K\alpha_2$-$L\alpha$ coincidence spectrum when the analysis was restricted to the $L\alpha$ range, indicating that the f_{23} value obtained in the conventional way is 3% low. When we add the effect of the broader satellite width, then altogether the analysis suggest that the conventionally obtained f_{23} value is 3–6 % low. To demonstrate the interplay between the $L\alpha$ and $L\beta_1$ tails and the background, the summed spectrum, together with the detector response function for the $L\alpha$ and $L\beta_1$ peaks and the constant background which was the result of the best fit, are presented in Fig. 8. We stress that this 3–6 % deviation was obtained using a very good quality detector; the difference is likely to be larger in the case of the more typical 180-eV resolution detectors used in past work, because these had substantially larger low-energy tails.

VI. DISCUSSION

In the two examples of this paper, it has been demonstrated that neglect of the proper spectral line shapes limits the accuracy of the determination of the f_{23} CK transition probabilities. Proper attention to the various lineshape effects would change measured values by amounts that exceed typically quoted experimental errors. In both experimental approaches, neglect of the various lineshape components will result in an underestimation of the f_{23} values when the $L_2L_3M_5$ channel is not allowed. When this channel is open, the coincidence method overestimates, while the photoionization method underestimates the f_{23} value. If experimental data reported in the literature had been evaluated according to the schemes outlined here, the resulting f_{23} values would have been in better agreement with theory [8]. The DHS theory therefore may be more successful than has formerly been apparent [2]. The deviation depends mainly on the evaluation methods and it could be averted to a large degree in future K-L coincidence studies by using more accurate detector response functions, taking into account the natural line shapes, and involving the satellites in the evaluation. However, the lack of information available for doubly ionized atomic transitions may be a limitation on such an analysis.

We found that the underestimate of f_{23} at atomic numbers below $Z=90$ is a little larger in the case of the synchrotron ionization method. This finding shows the same tendency as has been remarked upon in the comparison of the existing results from the two experimental methods [3]. Because the spectra encountered in the ionization approach are a blend of components from singly and doubly ionized atoms, we do not see a straightforward way to analyze them. From the current work we expect that the K-L coincidence method should give closer agreement with the theory.

This demonstrated dependence of f_{23} values upon the experimental technique and associated data analysis has further ramifications. For instance, if values of CK transition probabilities are to be used in the determination of the L subshell ionization cross sections in proton impact, it seems to us that the use of the parameters obtained by the synchrotron ionization method, assuming the analysis of the spectra is performed in a similar fashion to that of Jitschin and co-workers [2–4], might be more appropriate than the use of theoretical values or the values formerly given by the K-L coincidence method [5–7]. If data bases are to be constructed for x-ray emission analysis techniques (e.g., PIXE) whose data processing customarily ignores satellites and Lorentzian contributions, then perhaps they should use "effective" or "nominal" CK values based upon conventional data analysis that also ignores these aspects.

Finally, the satellites will affect also the data analysis in measurements of f_{13} in those atomic-number regions where the main decay channels are L_1-L_3M_4 and L_1-L_3M_5. These transitions together constitute some 70% of the overall transition rate for atomic numbers larger than 78 [14]. Although gold ($Z=79$) is the element most frequently chosen for inner-shell ionization and alignment studies, our current work suggests that this is an unfortunate choice because of the large correction factors caused by the CK transitions and the uncertainty in the latter. More reliable data might be obtained when the L_1-L_3M_i channels are energetically forbidden, for instance, around $Z=70$, where in addition the experimental and theoretical CK parameters are in better agreement.

ACKNOWLEDGMENTS

The current work was supported in part by the Natural Sciences and Enginerring Research Council of Canada and in part by the U.S. Department of Energy under Contract No. DE-AC05-84OR21400 with Martin Marietta Energy Systems, Inc.

[1] M. H. Chen, in *X-Ray and Inner-Shell Processes, Knoxville, 1990,* Proceedings of the Fifteenth International Conference on X-Ray and Inner-Shell Ionization (X90), Conf. Proc. No. 215, edited by T. A. Carlson, M. O. Krause, and S. T., Manson (AIP, New York, 1990), p. 391.

[2] W. Jitschin, G. Materlik, U. Werner, and P. Funke, J. Phys. B **18**, 1139 (1985).

[3] W. Jitschin, in *X-Ray and Inner-Shell Processes, Knoxville, 1990* (Ref. [1]), p. 408.

[4] R. Stotzel, U. Werner, M. Sarkar, and W. Jitschin, J. Phys. B **25**, 2295 (1992).

[5] J. L. Campbell, L. A. McNelles, J. S. Geiger, R. l. Graham, and J. S. Merritt, Can. J. Phys. **52**, 488 (1974); L. A. McNelles, J. L. Campbell, J. S. Geiger, R. L. Graham, and J. S. Merritt, *ibid.* **53**, 1349 (1975); J. L. Campbell and P. L. McGhee, J. Phys. B **21**, 2295 (1988).

[6] A. L. Catz, Phys. Rev. A **36**, 3155 (1987); **40**, 4977 (1989); A. L. Catz and M. F. Meyers, *ibid.*, **41**, 271 (1990).

[7] B. E. Gnade, R. A. Braga, and R. W. Fink, Phys. Rev. C **21**, 2025 (1980); **23**, 580 (1981).

[8] M. H. Chen, B. Crasemann, M. Aoyagi, and H. Mark, Phys. Rev. A **20**, 385 (1979); M. H. Chen, B. Crasemann, and H. Mark, *ibid.* **24**, 117 (1981).

[9] F. Parente, M. H. Chen, B. Crasemann, and H. Mark, At. Data Nucl. Data Tables **26**, 383 (1981).

[10] T. Papp, J. A. Maxwell, W. J. Teesdale, and J. L. Campbell, Phys. Rev. A **47**, 333 (1993).

[11] J. L. Campbell and J. X. Wang, X-Ray Spectrom. **20**, 191 (1991).

[12] T. Papp, J. L. Campbell, J. A. Maxwell, J.-X. Wang, and W. J. Teesdale, Phys. Rev. A **45**, 1711 (1992).

[13] J. L. Campbell, P. L. McGhee, R. R. Gingerich, R. W. Ollerhead, and J. A. Maxwell, Phys. Rev. A **30**, 161 (1984).

[14] M. H. Chen, B. Crasemann, and H. Mark, At. Data Nucl. Data Tables **24**, 13 (1979).

[15] L. Salgueiro, M. T. Ramos, M. L. Escrivao, M C. Martins, and J. G. Ferreira, J. Phys. B **7**, 342 (1974).

[16] W. Jitschin, J. Phys. B **17**, 4179 (1984).

[17] J. H. Scofield, *Atomic Inner-Shell Processes,* edited by B. Crasemann (Academic, New York, 1975), p. 265.

[18] J. Iihara, C. Izawa, T. Omori, and K. Yoshihara, Nucl. Instrum. Methods A **299**, 394 (1990).

[19] F. K. Richtmyer and E. G. Ramberg, Phys. Rev. **51**, 925 (1937).

[20] M. A. Blokhin and I. G. Svejcer, *Handbook of X-Ray Spectroscopy* (Nauka, Moscow, 1982).